

1 Ubiquitous production of branched glycerol dialkyl glycerol tetraethers (brGDGTs) in  
2 global marine environments: a new source indicator for brGDGTs

3 Wenjie Xiao<sup>1,2</sup>, Yinghui Wang<sup>2</sup>, Shangzhe Zhou<sup>2</sup>, Limin Hu<sup>3</sup>, Huan Yang<sup>4</sup>, Yunping Xu<sup>1,2\*</sup>

4 <sup>1</sup>Shanghai Engineering Research Center of Hadal Science and Technology, College of Marine  
5 Sciences, Shanghai Ocean University, Shanghai 201306, China

6 <sup>2</sup>MOE Key Laboratory for Earth Surface Process, College of Urban and Environmental Sciences,  
7 Peking University, Beijing 100871, China

8 <sup>3</sup>Key Laboratory of Marine Sedimentology and Environmental Geology, First Institute of  
9 Oceanography, State Oceanic Administration, Qingdao 266061, China

10 <sup>4</sup>State Key Laboratory of Biogeology and Environmental Geology, China University of Geosciences,  
11 Wuhan 430074, China

12 Corresponding author: Y Xu (ypxu@shou.edu.cn)

13

14 Abstract. Presumed source specificity of branched glycerol dialkyl glycerol tetraethers

15 (brGDGTs) from bacteria thriving in soil/peat and isoprenoid GDGTs (iGDGTs) from

16 aquatic organisms led to the development of several biomarker proxies for

17 biogeochemical cycle and paleoenvironment. However, recent studies reveal that

18 brGDGTs are also produced in aquatic environments besides soils and peat. Here we

19 examined three cores from the Bohai Sea and found distinct difference in brGDGT

20 compositions varying with the distance from the Yellow River mouth. We thus propose

21 an abundance ratio of hexamethylated to pentamethylated brGDGT (IIIa/IIa) to

22 evaluate brGDGT sources. The compilation of globally distributed 1354 marine

23 sediments and 589 soils shows that the IIIa/IIa ratio is generally <0.59 in soils, 0.59–

24 0.92 and >0.92 in marine sediments with and without significant terrestrial inputs,

25 respectively. Such disparity confirms the existence of two sources for brGDGTs, a

26 terrestrial origin with lower IIIa/IIa and a marine origin with higher IIIa/IIa, which is

27 likely attributed to generally higher pH and the production of brGDGTs in cold deep

28 water in sea. The application of the IIIa/IIa ratio to the East Siberian Arctic Shelf proves  
29 it a sensitive source indicator for brGDGTs, which is helpful for accurate estimation of  
30 organic carbon source and paleoclimates in marine settings.

31

## 32 1 Introduction

33 Glycerol dialkyl glycerol tetraethers (GDGTs), membrane lipids of archaea and  
34 certain bacteria, are widely distributed in marine and terrestrial environments  
35 (Reviewed by Schouten et al., 2013). These lipids have been a focus of attention of  
36 organic geochemists for more than ten years because they can be used to estimate  
37 environmental variables in the past such as temperature, soil pH, organic carbon source  
38 and microbial community structure (e.g., Schouten et al., 2002; Hopmans et al., 2004;  
39 Weijers et al., 2006; Lipp et al., 2008; Kim et al., 2010; Peterse et al., 2012; Zhu et al.,  
40 2016). There are generally two types of GDGTs, isoprenoid (iGDGTs) and non-  
41 isoprenoid, branched GDGTs (brGDGTs; Fig. 1). The former group is more abundant  
42 in aquatic settings and generally thought to be produced by Thaumarchaeota, a specific  
43 genetic cluster of the archaea domain (Sinninghe Damsté et al., 2002; Schouten et al.,  
44 2008), although Euryarchaeota may be a significant source of iGDGTs in the ocean  
45 (e.g., Lincoln et al., 2014). In contrast, the 1,2-di-*O*-alkyl-*sn*-glycerol configuration of  
46 brGDGTs was interpreted as an evidence for a bacterial rather than archaeal origin for  
47 brGDGTs (Sinninghe Damsté et al., 2000; Weijers et al., 2006). So far, only one  
48 brGDGT with two 13,16-dimethyl octacosanyl moieties was unambiguously detected  
49 in two species of Acidobacteria (Sinninghe Damsté et al., 2011), which hardly explains  
50 high diversity and ubiquitous occurrence of up to 15 brGDGT isomers in environments  
51 (Weijers et al., 2007b; De Jonge et al., 2014). Therefore, other biological sources of  
52 brGDGTs, although not yet identified, are likely.

53 The source difference between brGDGTs and iGDGTs led researchers to  
54 developing a branched and isoprenoid tetraether (BIT) index, expressed as relative  
55 abundance of terrestrial-derived brGDGTs to aquatic-derived Thaumarchaeota  
56 (Hopmans et al., 2004). Subsequent studies found that the BIT index is specific for soil

57 organic carbon because GDGTs are absent in vegetation (e.g., Walsh et al., 2008;  
58 Sparkes et al., 2015). The BIT index is generally higher than 0.9 in soils, but close to 0  
59 in marine sediments devoid of terrestrial inputs (Weijers et al., 2006; Weijers et al.,  
60 2014). Since its advent, the BIT index has been increasingly used to trace soil organic  
61 matter in different environments (e.g., Herfort et al., 2006; Kim et al., 2006; Blaga et  
62 al., 2011; Loomis et al., 2011; Wu et al., 2013). However, the BIT index is not just  
63 dependent on the abundance of brGDGTs, which reflects the input of soil organic matter,  
64 but also on the abundance of crenarchaeol, which is linked to marine productivity (e.g.,  
65 Herfort et al., 2006; Smith et al., 2010; Fietz et al., 2011). Besides the BIT index, Weijers  
66 et al. (2007b) found that the number of cyclopentane moieties of brGDGTs, expressed  
67 as Cyclization of Branched Tetraethers (CBT), correlated negatively with soil pH, while  
68 the number of methyl branches of brGDGTs, expressed as Methylation of Branched  
69 Tetraethers (MBT), was dependent on annual mean air temperature (MAT) and to a  
70 lesser extent on soil pH. The MBT/CBT proxies were further corroborated by  
71 subsequent studies (e.g., Sinninghe Damsté et al., 2008; Peterse et al., 2012; Yang et al.,  
72 2014a). Assuming that brGDGTs preserved in marine sediments close to the Congo  
73 River outflow were derived from soils in the river catchment, Weijers et al. (2007a)  
74 reconstructed large-scale continental temperature changes in tropical Africa that span  
75 the past 25,000 years by using the MBT/CBT proxy. Recently, De Jonge et al. (2013)  
76 used a tandem high performance liquid chromatography-mass spectrometry (2D  
77 HPLC-MS) and identified a series of novel 6-methyl brGDGTs which were previously  
78 coeluted with 5-methyl brGDGTs. This finding resulted in the redefinition and  
79 recalibration of brGDGTs' indexes (e.g., De Jonge et al., 2014; Xiao et al., 2015).

80 One underlying assumption of all brGDGT-based parameters is their source  
81 specificity, i.e., brGDGTs is only biosynthesized by bacteria thriving in soils and peat.  
82 Several studies, however, observed different brGDGT compositions between marine  
83 sediments and soils on adjacent lands, supporting in situ production of brGDGTs in  
84 marine environments (e.g., Peterse et al., 2009a; Zhu et al., 2011; Liu et al., 2014;  
85 Weijers et al., 2014; Zell et al., 2014), analogous to lacustrine settings (e.g., Sinninghe  
86 Damsté et al., 2009; Tierney & Russell, 2009; Tierney et al., 2012) and rivers (e.g., Zhu

87 et al., 2011; De Jonge et al., 2015; French et al., 2015; Zell et al., 2015). Peterse et al.  
88 (2009) compared the brGDGTs' distribution in Svalbard soils and nearby fjord  
89 sediments, and found that concentrations of brGDGTs (0.01–0.20  $\mu\text{g/g dw}$ ) in fjord  
90 sediments increased towards the open ocean and the distribution was strikingly different  
91 from that in soil. Zhu et al. (2011) examined distributions of GDGTs in surface  
92 sediments across a Yangtze River-dominated continental margin, and found evidence  
93 for production of brGDGTs in the oxic East China Sea shelf water column and the  
94 anoxic sediments/waters of the Lower Yangtze River. At the global scale, Fietz et al.  
95 (2012) reported a significant correlation between concentrations of brGDGTs and  
96 crenarchaeol ( $p < 0.01$ ;  $R^2 = 0.57\text{--}0.99$ ), suggesting that a common or mixed source for  
97 brGDGTs and iGDGTs are actually commonplace in lacustrine and marine settings.  
98 More recently, Sinninghe Damsté (2016) reported tetraethers in surface sediments from  
99 43 stations in the Berau River delta (Kalimantan, Indonesia), and this result, combined  
100 with data from other shelf systems, are coherent with the hypothesis that brGDGTs are  
101 in situ produced in shelf sediments especially at water depth of 50–300 m.

102 Fluvial inputs and wind are the most important pathways for transporting  
103 terrestrial material into sea. In continental shelf, fluvial discharge is more important  
104 because brGDGTs in atmospheric dust are either below the detection level (Hopmans  
105 et al., 2004) or present at low abundance (Fietz et al., 2013; Weijers et al., 2014). In the  
106 remote ocean where no direct impact from land erosion via rivers takes place, eolian  
107 transport and in situ production are major contributors for brGDGTs. Weijers et al.  
108 (2014) found that distributions of African dust-derived brGDGTs were similar to those  
109 of soils but different from those of distal marine sediments, providing a possibility to  
110 distinguish terrestrial vs. marine brGDGTs based on molecular compositions. However,  
111 so far no robust molecular indicator is available for estimating source of brGDGTs in  
112 marine environments. Considering this, we conduct a detailed study about GDGTs in  
113 three cores from the Bohai Sea which are subject to the Yellow River influence to  
114 different degree. Our purpose is to evaluate the source discerning capability of different  
115 brGDGT parameters, from which the most sensitive parameter is selected and applied

116 for globally distributed marine sediments and soils to test whether it is valid at the  
117 global scale. Our study supplies an important step for improving accuracy of brGDGT-  
118 derived proxies and better understanding the marine carbon cycle and  
119 paleoenvironments.

120

## 121 2 Material and methods

### 122 2.1 Study area and sampling

123 The Bohai Sea is a semi-enclosed shallow sea in northern China, extending about  
124 550 km from north to south and about 350 km from east to west. Its area is 77,000 km<sup>2</sup>  
125 and the mean depth is 18 m (Hu et al., 2009). The Bohai Strait at the eastern portion is  
126 the only passage connecting the Bohai Sea to the outer Yellow Sea. Several rivers,  
127 including Yellow River, the second largest river in the world in terms of sediment load  
128 (Milliman & Meade, 1983), drain into the Bohai Sea with a total annual runoff of  
129  $890 \times 10^8 \text{ m}^3$ . A 64 cm long gravity core (M1; 37.52°N, 119.32°E) was collected in July  
130 2011, while other two cores, M3 (38.66°N, 119.54°E; 53 cm long) and M7 (39.53°N,  
131 120.46°E; 60 cm long), were collected in July 2013 (Fig. 2). The sites M1, M3 and M7  
132 are located in the south, the center and the north of the Bohai Sea, respectively. The  
133 cores were transported to the lab where they were sectioned at 1 or 2 cm interval. The  
134 age model was established on basis of <sup>210</sup>Pb and <sup>137</sup>Cs activity, showing that the bottom  
135 sediments are less than 100 years old (Wu et al., 2013 and unpublished data).

136

### 137 2.2 Lipid extraction and analyses

138 The detailed procedures for lipid extraction and GDGT analyses have been  
139 described in previous studies (Ding et al., 2015; Xiao et al., 2015). Briefly, the  
140 homogenous freeze-dried samples were ultrasonically extracted with dichloromethane  
141 (DCM)/methanol (3:1 v:v). The extracts were separated into nonpolar and polar fraction  
142 over silica gel columns. The latter fraction containing GDGTs was analyzed using an  
143 Agilent 1200 HPLC-atmospheric pressure chemical ionization-triple quadruple mass  
144 spectrometry (HPLC-APCI-MS) system. The separation of 5- and 6-methyl brGDGTs  
145 was achieved with two silica columns in sequence (150 mm×2.1 mm; 1.9 μm, Thermo

146 Finnigan; USA). The quantification was achieved by comparison of the respective  
147 protonated ion peak areas of each GDGT to the internal standard (C<sub>46</sub> GDGT) in  
148 selected ion monitoring (SIM) mode. The protonated ions were m/z 1050, 1048, 1046,  
149 1036, 1034, 1032, 1022, 1020, 1018 for brGDGTs, 1302, 1300, 1298, 1296, 1292 for  
150 iGDGTs and 744 for C<sub>46</sub> GDGT.

151

### 152 2.3 Parameter calculation and statistics

153 The BIT, MBT, Methyl Index (MI), Degree of Cyclization (DC) of brGDGTs and  
154 weighted average number of cyclopentane moieties for tetramethylated brGDGTs  
155 (#Rings<sub>tetra</sub>) were calculated according to the definitions of Hopmans et al. (2004),  
156 Weijers et al. (2007b), Zhang et al. (2011), Sinninghe Damsté et al. (2009) and  
157 Sinninghe Damsté (2016), respectively.

$$158 \text{ BIT} = \frac{\text{Ia} + \text{IIa} + \text{IIIa}}{\text{Ia} + \text{IIa} + \text{IIIa} + \text{IV}} \quad (1)$$

$$159 \text{ MBT} = \frac{\text{Ia} + \text{Ib} + \text{Ic}}{\text{Ia} + \text{IIa} + \text{IIIa} + \text{Ib} + \text{IIb} + \text{IIIb} + \text{Ic} + \text{IIc} + \text{IIIc}} \quad (2)$$

$$160 \text{ MI} = 4 \times (\text{Ia} + \text{Ib} + \text{Ic}) + 5 \times (\text{IIa} + \text{IIb} + \text{IIc}) + 6 \times (\text{IIIa} + \text{IIIb} + \text{IIIc}) \quad (3)$$

$$161 \text{ DC} = \frac{\text{Ib} + \text{IIb}}{\text{Ia} + \text{IIa} + \text{Ib} + \text{IIb}} \quad (4)$$

$$162 \text{ \#Rings}_{\text{tetra}} = \frac{\text{Ib} + 2 \times \text{Ic}}{\text{Ia} + \text{Ib} + \text{Ic}} \quad (5)$$

163 where roman numbers denote relative abundance of compounds depicted in Fig. 1. In  
164 this study, we used two silica LC columns in tandem and successfully separated 5- and  
165 6-methyl brGDGTs. However, many previous studies (e.g., Weijers et al., 2006) used  
166 one LC column and did not separate 5- and 6-methyl brGDGTs. Considering this, we  
167 combined 5-methyl and 6-methyl brGDGT as one compound in this study, for example,  
168 IIIa denotes the total abundance of brGDGT IIIa and IIIa' in figure 1.

169 An analysis of variance (ANOVA) was conducted for different types of samples  
170 to determine if they differ significantly from each other. The SPSS 16.0 software  
171 package (IBM, USA) was used for the statistical analysis. Squared Pearson correlation  
172 coefficients (R<sup>2</sup>) were reported and a significance level is  $p < 0.05$ .

173

## 174 2.4 Data compilation of global soils and marine sediments

175 The dataset in this study are composed of **relative abundance of GDGTs and**  
176 **derived parameters** from 1354 globally distributed soils and 589 marine sediments (Fig.  
177 2 and supplementary data). These sampling sites span a wide area from 75.00°S to  
178 79.28°N and 168.08°W to 174.40°E **and the water depth ranges from 1.0 to 5521 m.**  
179 The marine samples are from the South China Sea (Hu et al., 2012; Jia et al., 2012;  
180 O'Brien et al., 2014; Dong et al., 2015), Caribbean Sea (O'Brien et al., 2014), western  
181 equatorial Pacific Ocean (O'Brien et al., 2014), southeast Pacific Ocean (Kaiser et al.,  
182 2015), the Chukchi and Alaskan Beaufort Seas (Belicka & Harvey, 2009), eastern  
183 Indian Ocean (Chen et al., 2014), East Siberian Arctic Shelf (Sparkes et al., 2015), Kara  
184 Sea (De Jonge et al., 2015; De Jonge et al., 2016), Svalbard fjord (Peterse et al., 2009a),  
185 Red Sea (Trommer et al., 2009), the southern Adriatic Sea (Leider et al., 2010),  
186 Columbia estuary (French et al., 2015), globally distributed distal marine sediments  
187 (Weijers et al., 2014) and the Bohai Sea (this study). Soil samples are from the Svalbard  
188 (Peterse et al., 2009b), Columbia (French et al., 2015), China (Yang et al., 2013; Yang  
189 et al., 2014a; Yang et al., 2014b; Ding et al., 2015; Xiao et al., 2015; Hu et al., 2016),  
190 globally distributed soils (Weijers et al., 2006; Peterse et al., 2012; De Jonge et al.,  
191 2014), California geothermal (Peterse et al., 2009b), France and Brazil (Huguet et al.,  
192 2010), western Uganda (Loomis et al., 2011), the USA (Tierney et al., 2012), Tanzania  
193 (Coffinet et al., 2014), Indonesian, Vietnamese, Philippine, China and Italia (Mueller-  
194 Niggemann et al., 2016).

195

## 196 3 Results and discussion

### 197 3.1 Distribution and source of brGDGTs in Bohai Sea

198 **A series of iGDGTs including crenarchaeol and brGDGTs including 5-methyl and**  
199 **6-methyl isomers were detected in Bohai Sea sediments.** For brGDGTs, a total of 15  
200 compounds were identified including three tetramethylated brGDGTs (Ia, Ib and Ic),  
201 six pentamethylated brGDGTs (IIa, IIb, IIc, IIa', IIb' and IIc') and six hexamethylated  
202 brGDGTs (IIIa, IIIb, IIIc, IIIa', IIIb' and IIIc'). In order to evaluate provenances of  
203 brGDGTs, we calculated various parameters including the BIT index, percentages of

204 tetra-, penta- and hexa-methylated brGDGTs, #rings for tetramethylated brGDGTs, DC,  
205 MI, MBT, brGDGTs IIIa/IIa and Ia/IIa (Table 1). The values of the BIT index ranged  
206 from 0.27 to 0.76 in the core M1, which are much higher than that in the core M3 (0.04–  
207 0.25) and the core M7 (0.04–0.18). Such difference is not surprising since the site M1  
208 is closest to the Yellow River outflow, and receives more terrestrial organic carbon than  
209 other two sites (Fig. 2). However, the BIT index itself has no ability to determine the  
210 source of brGDGTs (terrestrial vs. aquatic) because brGDGTs and crenarchaeol used in  
211 this index are thought to be specific for soil organic carbon and marine organic carbon,  
212 respectively (Hopmans et al., 2004), although crenarchaeol is also present in soils at  
213 low abundance (Weijers et al., 2006). For individual brGDGTs, the core M1 is  
214 characterized by significantly higher percentage of brGDGT IIa (28±1%) than the core  
215 M2 (18±1%) and the core M3 (18±0%; Fig. 3). We performed ANOVA for a variety of  
216 brGDGTs' parameters. All results except from MI show a significant difference  
217 between Chinese soils and Bohai Sea sediments. The IIIa/IIa ratio is the most sensitive  
218 parameter which can completely separate the samples into four groups: Chinese soils  
219 (0.39±0.25; Mean±SD; same hereafter), M1 sediments (0.63±0.06), M3 sediments  
220 (1.16±0.12) and M7 sediments (0.93±0.07).

221 Three factors may account for the occurrence of higher IIIa/IIa ratio in the Bohai  
222 Sea sediments than Chinese soils: selective degradation during land to sea transport,  
223 admixture of river produced brGDGTs and in situ production of brGDGTs in sea.  
224 Huguet et al. (2008; 2009) reported that iGDGTs (i.e., crenarchaeol) was degraded at a  
225 rate of 2-fold higher than soil derived brGDGTs under long term oxygen exposure in  
226 the Madeira Abyssal Plain, leading to increase of the BIT index. Such selective  
227 degradation, however, cannot explain significant different IIIa/IIa ratio between the  
228 Chinese soils and Bohai Sea sediments because unlike crenarchaeol, both IIIa and IIa  
229 belong to brGDGTs with similar chemical structures and thus have similar degradation  
230 rates. In situ production of brGDGTs in rivers is a widespread phenomenon, and can  
231 change brGDGTs' composition in sea when they were transported there (e.g., Zhu et al.,  
232 2011; De Jonge et al., 2015; Zell et al., 2015). However, this effect is minor in the  
233 Yellow River because extremely high turbidity (up to 220 kg/m<sup>3</sup> during the flood season;



234 Ren & Shi, 1986) greatly constrain the growth of aquatic organisms. The studies along  
235 lower Yellow River-estuary-coast transect suggested that brGDGTs in surface  
236 sediments were primarily a land origin (Wu et al., 2014). In our study, the site M1 is  
237 adjacent to the Yellow River mouth and receives the largest amount of terrestrial organic  
238 matter, causing lower IIIa/IIa values ( $0.63\pm 0.06$ ). In contrast, the site M3 located in  
239 central Bohai Sea comprises of the least amount of terrestrial organic matter, resulting  
240 in higher IIIa/IIa values ( $1.16\pm 0.12$ ). The intermediate IIIa/IIa values at the site M7  
241 ( $0.93\pm 0.07$ ) is attributed to moderate land erosion nearby northern Bohai Sea (Fig. 2).  
242 These GDGTs' results, consistent with other terrestrial biomarkers such as C<sub>29</sub> and C<sub>31</sub>  
243 *n*-alkanes and C<sub>29</sub> sterol (data not showed here), suggest that the higher IIIa/IIa values  
244 in the Bohai Sea sediments compared to Chinese soils ( $0.39\pm 0.25$ ) is most likely caused  
245 by in situ production of brGDGTs.

246

247

### 248 3.2 Regional and global validation of brGDGT IIIa/IIa

249 To test whether the IIIa/IIa ratio is valid in other environments, we apply it to the  
250 Svalbard (Peterse et al., 2009a), the Yenisei River outflow (De Jonge et al., 2015) and  
251 the East Siberian Arctic Shelf (Sparkes et al., 2015). Similar to Bohai Sea in this study,  
252 the compounds brGDGT IIa and IIIa are also ubiquitously present in these  
253 environments. By comparing the compositions of brGDGTs in Svalbard soils and  
254 nearby fjord sediments, Peterse et al. (2009a) indicated that sedimentary organic matter  
255 in fjords was predominantly a marine origin. A plot of BIT vs. IIIa/IIa (Fig. 4a) clearly  
256 grouped the samples into two groups which correspond to soils ( $>0.75$  for BIT and  $<1.0$   
257 for IIIa/IIa) and marine sediments ( $<0.3$  for BIT and  $>1.0$  for IIIa/IIa). Another line of  
258 evidence is from De Jonge et al. (2015) who examined brGDGTs in core lipids (CLs)  
259 and intact polar lipids (IPLs) in the Yenisei River outflow. As the IPLs are rapidly  
260 degraded in the environment, they can be used to trace living or recently living material,  
261 while the CLs are generated via degradation of the IPLs after cell death (White et al.,  
262 1979; Lipp et al., 2008). The compilation of brGDGTs' abundance from De Jonge et al.  
263 (2015) shows significant difference of the IIIa/IIa ratio between the IPL fractions ( $>1.0$ )

264 and CL fractions ( $<0.8$ ; Fig. 4b). Such disparity supports that brGDGTs produced in  
265 marine environments have higher IIIa/IIa values because labile intact polar brGDGTs  
266 are mainly produced in situ, whereas recalcitrant core brGDGTs are composed of more  
267 allochthonous terrestrial components. Sparkes et al. (2015) examined brGDGTs in  
268 surface sediments across the East Siberian Arctic Shelf (ESAS) including the Dmitry-  
269 Laptev Strait, Buor-Khaya Bay, ESAS nearshore and ESAS offshore. The plot of BIT  
270 vs. IIIa/IIa again results into two groups, one group with lower BIT values ( $<0.3$ ) and  
271 higher IIIa/IIa values (0.8–2.3) mainly from ESAS offshore, and another group with  
272 higher BIT values (0.3–1.0) and lower IIIa/IIa values (0.4–0.9) from the Dmitry-Laptev  
273 Strait, Buor-Khaya Bay and ESAS nearshore (Fig. 4c). A strong linear correlation was  
274 observed between the IIIa/IIa ratio and the distance from river mouth ( $R^2=0.58$ ;  $p<0.05$ ;  
275 Fig. 4d), in accord with the data of the BIT index and  $\delta^{13}C_{org}$  (Sparkes et al., 2015). All  
276 lines of evidence support that marine-derived brGDGTs have higher IIIa/IIa values than  
277 terrestrial derived brGDGTs.

278 We further extend the dataset on global scale (Fig. 5), showing that the IIIa/IIa  
279 ratio is still significantly higher in marine sediments than soils ( $p < 0.01$ ). An exception  
280 was observed for Red Sea sediments which have unusually low IIIa/IIa values  
281 ( $0.39\pm 0.21$ ) compared to other marine sediments ( $>0.87$ ). The Red Sea has a restricted  
282 connection to the Indian Ocean via the Bab el Mandeb Strait. This, combined with high  
283 insolation, low precipitation and strong winds result in surface water salinity up to 41  
284 PSU in the south and 36 PSU in the north of the Red Sea (Sofianos et al., 2002). Under  
285 such extreme environment, distinct microbial populations may be developed and  
286 produced GDGTs different from that in other marine settings (See Trommer et al., 2009  
287 for details).

288 Overall, the global distribution of IIIa/IIa presents the highest values in many deep  
289 sea sediments (2.6–5.1), the lowest values in soils ( $<1.0$ ), and intermediate values in  
290 sediments from bays, coastal areas or marginal seas (0.87–2.62; Fig. 5). These results  
291 are consistent with our data from the Bohai Sea, and confirm that the IIIa/IIa ratio is a  
292 useful proxy for tracing the source of brGDGTs in marine sediments at regional and  
293 global scales.

294 **Why do marine sediments generally have higher IIIa/IIa values than soils?** It has  
295 been reported that relative number of methyl groups positively correlates with soil pH  
296 and negatively correlates with MAT (Weijers et al., 2007b; Peterse et al., 2012). The  
297 IIIa/IIa ratio is actually an abundance ratio of hexamethylated to pentamethylated  
298 brGDGT, and thus is also affected by ambient temperature and pH. Unlike iGDGTs  
299 which is well known to be mainly produced by Thaumarchaeota (Sinninghe Damsté et  
300 al., 2002; Schouten et al., 2008), the marine source of brGDGTs remains elusive. Here,  
301 we assume that marine organisms producing brGDGTs response to ambient  
302 temperature in the same way as those soil bacteria producing brGDGTs, i.e., a negative  
303 correlation between relative number of methyl group of brGDGTs and ambient  
304 temperature. Because a large temperature gradient exists from surface to bottom water  
305 in ocean, we need consider the locale where brGDGTs are produced. If brGDGTs in  
306 marine environments are predominantly produced in euphotic zone, we would not  
307 observe a significant difference for the IIIa/IIa ratio between land and sea because both  
308 soils and marine sediments are globally distributed, leading to no systematic difference  
309 between soil temperature and sea surface temperature. Alternatively, if brGDGTs in  
310 marine sediments are partially derived from deep-water dwelling or benthic organisms,  
311 cold deep water (generally 1–2 °C) would cause higher IIIa/IIa values in marine  
312 sediments, as we observed in this study. Although to the best of our knowledge, there  
313 is no study reporting in situ production of brGDGTs throughout water column in ocean.  
314 Recent studies (Taylor et al., 2013; Kim et al., 2015) have suggested that  
315 Thaumarchaeota thriving in the deeper, bathypelagic water-column (>1000 m water  
316 depth) biosynthesized iGDGTs with different compositions as surface dwelling  
317 Thaumarchaeota, and thereby alter signals of TEX<sub>86</sub> in sediments. Besides temperature,  
318 pH can also alter compositions of brGDGTs (Weijers et al., 2007). Based on global soil  
319 data, the IIIa/IIa ratio shows a strong positive correlation with soil pH ( $R^2=0.51$ ; Fig.  
320 6). In our study, the majority of soils are acidic or neutral (pH<7.3) and only 8% of soil  
321 samples mainly from semi-arid and arid regions have pH of >8.0 (e.g., Yang et al., 2014a).  
322 In contrast, seawater is constantly alkaline with a mean pH of 8.2. With this systematic  
323 difference, bacteria living in soils tend to produce higher proportions of brGDGT IIa,

324 whereas unknown marine organisms tend to biosynthesize higher proportions of  
325 brGDGT IIIa if they response to ambient pH in a similar way as soil bacteria in term of  
326 biosynthesis of brGDGTs. It should be pointed out that unlike fairly stable pH of  
327 overlying sea water, the pH of pore waters in marine sediments can vary significantly, which  
328 may influence compositions of brGDGTs. Nevertheless, at current stage, the occurrence of  
329 higher IIIa/IIa values in marine sediments is most likely attributed to relatively higher  
330 pH and lower deep water temperature. Further studies are needed to disentangle relative  
331 importance of these two factors.

332

### 333 3.3 Implication of IIIa/IIa on other brGDGT proxies

334 Because brGDGTs can be produced in marine settings, they are no longer specific  
335 for soil organic matter, which inevitably affects brGDGT proxies (e.g., BIT, MBT/CBT).  
336 The plot of BIT vs. IIIa/IIa on basis of global dataset shows that the IIIa/IIa ratio has  
337 the value of <0.59 for 90% of soil samples and >0.92 for 90% of marine sediments (Fig.  
338 7). Considering this fact, we propose that the IIIa/IIa ratio of <0.59 and >0.92 represents  
339 terrestrial (or soil) and marine endmembers, respectively. The BIT index has the value  
340 of >0.67 for 90% of soils and <0.16 for 90% of marine sediments (Fig. 7). Overall, the  
341 BIT index decreased with increasing IIIa/IIa values ( $BIT = 1.08 \times 0.28^{\frac{IIIa}{IIa}} -$   
342  $0.03; R^2 = 0.77; Fig. 7$ ), suggesting that both the IIIa/IIa and BIT are useful indexes  
343 for assessing soil organic carbon in marine settings. However, when the BIT index has  
344 an intermediate value (i.e., 0.16 to 0.67), it is not valid to determine the provenance of  
345 brGDGTs. For example, several marine samples having BIT values of ~0.35 show a  
346 large range of IIIa/IIa (0.4 to 2.4; Fig. 7), suggesting that the source of brGDGTs can  
347 vary case by case. Under this situation, the measurement of the IIIa/IIa ratio is strongly  
348 recommended.

349 The different IIIa/IIa values between land and marine endmembers may supply an  
350 approach to quantify the contribution of soil organic carbon in marine sediments.  
351 Similar to the BIT index, we used a binary mixing model to calculate percentage of soil  
352 organic carbon (%OC<sub>soil</sub>) as follow:

$$353 \quad \%OC_{\text{soil}} = \left[ \frac{[\text{IIIa/IIa}]_{\text{sample}} - [\text{IIIa/IIa}]_{\text{marine}}}{[\text{IIIa/IIa}]_{\text{soil}} - [\text{IIIa/IIa}]_{\text{marine}}} \right] * 100 \quad (6)$$

354 Where  $[\text{IIIa/IIa}]_{\text{sample}}$ ,  $[\text{IIIa/IIa}]_{\text{soil}}$  and  $[\text{IIIa/IIa}]_{\text{marine}}$  are the abundance ratio of brGDGT  
 355 IIIa/IIa for samples, soils and marine sediments devoid of terrestrial influences,  
 356 respectively.

357 We applied this binary mixing model to the East Siberian Arctic Shelf because the  
 358 data of BIT,  $\delta^{13}\text{C}_{\text{org}}$  and distance from river mouth are all available (Sparkes et al., 2015).  
 359 With the distance from river mouth increasing from 25 to >700 km, the BIT, IIIa/IIa  
 360 and  $\delta^{13}\text{C}_{\text{org}}$  change from 0.95 to 0, 0.53 to 2.21 and  $-27.4\text{‰}$  to  $-21.2\text{‰}$ , respectively,  
 361 reflecting spatial variability of sedimentary organic carbon sources. For the BIT index,  
 362 we used 0.97 and 0.01 as terrestrial and marine endmember values based on previous  
 363 studies for Arctic surrounding regions (De Jonge et al., 2014; Peterse et al., 2014),  
 364 which are similar to global average values (Hopmans et al., 2004). For  $\delta^{13}\text{C}_{\text{org}}$ , we chose  
 365  $-27\text{‰}$  and  $-20\text{‰}$  as C3 terrestrial and marine organic carbon endmembers (Meyers,  
 366 1997). For the IIIa/IIa ratio, we used a global average value of marine sediments (1.6)  
 367 and soils (0.24), respectively, based on this study. By applying these endmember values  
 368 into Eq. 6, we calculated percentage of soil organic carbon ( $\%OC_{\text{soil}}$ ). We removed a  
 369 few data points if their calculated  $\%OC_{\text{soil}}$  were greater than 100% or below 0%. It  
 370 should be noted that the endmember value will affect quantitative results, but does not  
 371 change a general trend of  $\%OC_{\text{soil}}$ . The results based on all three parameters show a  
 372 decreasing trend seawards (Fig. 8). However, the  $\%OC_{\text{soil}}$  based on  $\delta^{13}\text{C}_{\text{org}}$  is the highest  
 373 ( $75\pm 18\%$ ), followed by that from the IIIa/IIa ratio ( $58\pm 15\%$ ) and then that from the BIT  
 374 index ( $43\pm 27\%$ ). This difference have been explained by that  $\delta^{13}\text{C}_{\text{org}}$  is a bulk proxy for  
 375 marine vs. terrestrial influence of sedimentary organic carbon (SOC), whereas the BIT  
 376 index is for a portion of the bulk SOC, i.e., soil OC (Walsh et al., 2008) or fluvial OC  
 377 (Sparkes et al., 2015). For the estimated  $\%OC_{\text{soil}}$ ,  $\delta^{13}\text{C}_{\text{org}}$  presents a stronger positive  
 378 correlation with the IIIa/IIa ratio ( $R^2=0.49$ ) than the BIT index ( $R^2=0.45$ ), suggesting  
 379 that the IIIa/IIa ratio may serve a better proxy for quantifying soil organic carbon than  
 380 the BIT index because it is less affected by selective degradation of branched vs.  
 381 isoprenoid GDGTs and high production of crenarchaea in marine environments (Smith

382 et al., 2012).

383

#### 384 4 Conclusions

385 Our investigation in brGDGTs in three Bohai Sea cores and globally distributed  
386 soils and marine sediments shows that the brGDGTs IIIa/IIa ratio is lower than 0.59 in  
387 90% of soils, but higher than 0.92 in 90% of marine sediments devoid of significant  
388 terrestrial inputs, supporting that the IIIa/IIa is a sensitive proxy for assessing soil vs.  
389 marine derived brGDGTs at regional and global scales. The in situ production of  
390 brGDGTs in marine environments is a ubiquitous phenomenon, which is particularly  
391 important for those marine sediments with low BIT index ( $<0.16$ ) where brGDGTs are  
392 exclusively of a marine origin. A systemic difference of the IIIa/IIa value between soils  
393 and marine sediments reflects an influence of pH rather than temperature on the  
394 biosynthesis of brGDGTs by source organisms. Given these facts, we recommend to  
395 calculate the IIIa/IIa ratio before estimating organic carbon source, paleo-soil pH and  
396 MAT based on the BIT and MBT/CBT proxies. We also note a relatively large scatter  
397 of the IIIa/IIa ratio within both terrestrial and marine realms, and recently reported  
398 different environmental responses of 5-methyl vs. 6-methyl brGDGTs (e.g., De Jonge  
399 et al., 2014, 2016; Xiao et al., 2015). As a result, the separation of these two types of  
400 isomers is needed in future studies in order to develop more accurate brGDGTs-based  
401 proxies.

402

403 *Acknowledgements.* The work was financially supported by the National Science  
404 Foundation of China (41476062). We are grateful for X. Dang for GDGT analyses. G.  
405 Jia, J. Hu, A. Leider, G. Mollenhauer, G. Trommer and R. Smith are thanked for kindly  
406 supplying GDGT data. Dr. Ding He and two anonymous reviewers are thanked for  
407 constructive comments.

408

#### 409 References

410 Belicka, L.L., Harvey, H.R., The sequestration of terrestrial organic carbon in Arctic Ocean sediments:  
411 A comparison of methods and implications for regional carbon budgets. *Geochim. Cosmochim.*

412 Acta, 73, 6231–6248, 2009.

413 Blaga, C.I., Reichart, G.J., Vissers, E.W., Lotter, A.F., Anselmetti, F.S., Damste, J.S.S., Seasonal changes  
414 in glycerol dialkyl glycerol tetraether concentrations and fluxes in a perialpine lake:  
415 Implications for the use of the TEX<sub>86</sub> and BIT proxies. *Geochim. Cosmochim. Acta*, 75, 6416–  
416 6428, 2011.

417 Chen, W., Mohtadi, M., Schefuß, E., Mollenhauer, G., Organic-geochemical proxies of sea surface  
418 temperature in surface sediments of the tropical eastern Indian Ocean. *Deep Sea Research Part*  
419 *I: Oceanographic Research Papers*, 88, 17–29, 2014.

420 Coffinet, S., Hugué, A., Williamson, D., Fosse, C., Derenne, S., Potential of GDGTs as a temperature  
421 proxy along an altitudinal transect at Mount Rungwe (Tanzania). *Org. Geochem.*, 68, 82–89,  
422 2014.

423 De Jonge, C., Hopmans, E.C., Stadnitskaia, A., Rijpstra, W.I.C., Hofland, R., Tegelaar, E., Sinninghe  
424 Damsté, J.S., Identification of novel penta- and hexamethylated branched glycerol dialkyl  
425 glycerol tetraethers in peat using HPLC–MS2, GC–MS and GC–SMB-MS. *Org. Geochem.*, 54,  
426 78–82, 2013.

427 De Jonge, C., Hopmans, E.C., Zell, C.I., Kim, J.-H., Schouten, S., Sinninghe Damsté, J.S., Occurrence  
428 and abundance of 6-methyl branched glycerol dialkyl glycerol tetraethers in soils: Implications  
429 for palaeoclimate reconstruction. *Geochim. Cosmochim. Acta*, 141, 97–112, 2014.

430 De Jonge, C., Stadnitskaia, A., Cherkashov, G., Sinninghe Damsté, J.S., Branched glycerol dialkyl  
431 glycerol tetraethers and crenarchaeol record post-glacial sea level rise and shift in source of  
432 terrigenous brGDGTs in the Kara Sea (Arctic Ocean). *Org. Geochem.*, 92, 42–54, 2016.

433 De Jonge, C., Stadnitskaia, A., Hopmans, E.C., Cherkashov, G., Fedotov, A., Streletskaya, I.D., Vasiliev,  
434 A.A., Sinninghe Damsté, J.S., Drastic changes in the distribution of branched tetraether lipids  
435 in suspended matter and sediments from the Yenisei River and Kara Sea (Siberia): Implications  
436 for the use of brGDGT-based proxies in coastal marine sediments. *Geochim. Cosmochim. Acta*,  
437 165, 200–225, 2015.

438 Ding, S., Xu, Y., Wang, Y., He, Y., Hou, J., Chen, L., He, J.S., Distribution of branched glycerol dialkyl  
439 glycerol tetraethers in surface soils of the Qinghai–Tibetan Plateau: implications of brGDGTs-  
440 based proxies in cold and dry regions. *Biogeosciences*, 12, 3141–3151, 2015.

441 Dong, L., Li, Q., Li, L., Zhang, C.L., Glacial–interglacial contrast in MBT/CBT proxies in the South

442 China Sea: Implications for marine production of branched GDGTs and continental  
443 teleconnection. *Org. Geochem.*, 79, 74–82, 2015.

444 Fietz, S., Huguet, C., Bendle, J., Escala, M., Gallacher, C., Herfort, L., Jamieson, R., Martínez-García,  
445 A., McClymont, E.L., Peck, V.L., Prahl, F.G., Rossi, S., Rueda, G., Sanson-Barrera, A., Rosell-  
446 Melé, A., Co-variation of crenarchaeol and branched GDGTs in globally-distributed marine and  
447 freshwater sedimentary archives. *Glob. Planet. Change*, 92, 275-285, 2012.

448 Fietz, S., Prahl, F.G., Moraleda, N., Rosell-Melé, A., Eolian transport of glycerol dialkyl glycerol  
449 tetraethers (GDGTs) off northwest Africa. *Org. Geochem.*, 64, 112–118, 2013.

450 French, D.W., Huguet, C., Turich, C., Wakeham, S.G., Carlson, L.T., Ingalls, A.E., Spatial distributions  
451 of core and intact glycerol dialkyl glycerol tetraethers (GDGTs) in the Columbia River Basin  
452 and Willapa Bay, Washington: Insights into origin and implications for the BIT index. *Org.*  
453 *Geochem.*, 88, 91–112, 2015.

454 Herfort, L., Schouten, S., Boon, J.P., Woltering, M., Baas, M., Weijers, J.W.H., Damsté, J.S.S.,  
455 Characterization of transport and deposition of terrestrial organic matter in the southern North  
456 Sea using the BIT index. *Limnol. Oceanogr.*, 51, 2196 – 2205, 2006.

457 Hopmans, E.C., Weijers, J.W.H., Schefuss, E., Herfort, L., Damste, J.S.S., Schouten, S., A novel proxy  
458 for terrestrial organic matter in sediments based on branched and isoprenoid tetraether lipids.  
459 *Earth Planet. Sci. Lett.*, 224, 107–116, 2004.

460 Hu, J., Meyers, P.A., Chen, G., Peng, P.A., Yang, Q., Archaeal and bacterial glycerol dialkyl glycerol  
461 tetraethers in sediments from the Eastern Lau Spreading Center, South Pacific Ocean. *Org.*  
462 *Geochem.*, 43, 162–167, 2012.

463 Hu, J., Zhou, H., Peng, P.A., Spiro, B., Seasonal variability in concentrations and fluxes of glycerol  
464 dialkyl glycerol tetraethers in Huguangyan Maar Lake, SE China: Implications for the  
465 applicability of the MBT–CBT paleotemperature proxy in lacustrine settings. *Chem. Geol.*, 420,  
466 200-212, 2016.

467 Hu, L., Guo, Z., Feng, J., Yang, Z., Fang, M., Distributions and sources of bulk organic matter and  
468 aliphatic hydrocarbons in surface sediments of the Bohai Sea, China. *Mar. Chem.*, 113, 197–  
469 211, 2009.

470 Huguet, A., Fosse, C., Metzger, P., Fritsch, E., Derenne, S., Occurrence and distribution of extractable  
471 glycerol dialkyl glycerol tetraethers in podzols. *Org. Geochem.*, 41, 291–301, 2010.



472 Huguet, C., de Lange, G.J., Gustafsson, Ö., Middelburg, J.J., Sinninghe Damsté, J.S., Schouten, S.,  
473 Selective preservation of soil organic matter in oxidized marine sediments (Madeira Abyssal  
474 Plain). *Geochim. Cosmochim. Acta*, 72, 6061–6068, 2008.

475 Huguet, C., Kim, J.-H., de Lange, G.J., Sinninghe Damsté, J.S., Schouten, S., Effects of long term oxic  
476 degradation on the , TEX<sub>86</sub> and BIT organic proxies. *Org. Geochem.*, 40, 1188–1194, 2009.

477 Jia, G., Zhang, J., Chen, J., Peng, P.A., Zhang, C.L., Archaeal tetraether lipids record subsurface water  
478 temperature in the South China Sea. *Org. Geochem.*, 50, 68–77, 2012.

479 Kaiser, J., Schouten, S., Kilian, R., Arz, H.W., Lamy, F., Sinninghe Damsté, J.S., Isoprenoid and branched  
480 GDGT-based proxies for surface sediments from marine, fjord and lake environments in Chile.  
481 *Org. Geochem.*, 89, 117–127, 2015.

482 Kim, J.-H., Schouten, S., Rodrigo-Gámiz, M., Rampen, S., Marino, G., Huguet, C., Helmke, P., Buscail,  
483 R., Hopmans, E.C., Pross, J., Sangiorgi, F., Middelburg, J.B.M., Sinninghe Damsté, J.S.,  
484 Influence of deep-water derived isoprenoid tetraether lipids on the paleothermometer in the  
485 Mediterranean Sea. *Geochim. Cosmochim. Acta*, 150, 125-141, 2015.

486 Kim, J.H., Meer, J.V.D., Schouten, S., Helmke, P., Willmott, V., Sangiorgi, F., Koç, N., Hopmans, E.C.,  
487 Damsté, J.S.S., New indices and calibrations derived from the distribution of crenarchaeal  
488 isoprenoid tetraether lipids: Implications for past sea surface temperature reconstructions.  
489 *Geochim. Cosmochim. Acta*, 74, 4639–4654, 2010.

490 Kim, J.H., Schouten, S., Buscail, R., Ludwig, W., Bonnin, J., Sinninghe Damsté, J.S., Bourrin, F., Origin  
491 and distribution of terrestrial organic matter in the NW Mediterranean (Gulf of Lions):  
492 Exploring the newly developed BIT index. *Geochem. Geophys. Geosy.*, 7, 220–222, 2006.

493 Leider, A., Hinrichs, K.U., Mollenhauer, G., Versteegh, G.J.M., Core-top calibration of the lipid-based  
494 UK'37 and TEX<sub>86</sub> temperature proxies on the southern Italian shelf (SW Adriatic Sea, Gulf of  
495 Taranto). *Earth Planet. Sci. Lett.*, 300, 112–124, 2010.

496 Lincoln, S.A., Wai, B., Eppley, J.M., Church, M.J., Summons, R.E., Delong, E.F., Planktonic  
497 Euryarchaeota are a significant source of archaeal tetraether lipids in the ocean. *Proc. Natl. Acad.*  
498 *Sci.*, 111, 9858–9863, 2014.

499 Lipp, J.S., Morono, Y., Inagaki, F., Hinrichs, K.U., Significant contribution of Archaea to extant biomass  
500 in marine subsurface sediments. *Nature*, 454, 991–994, 2008.

501 Liu, X.-L., Zhu, C., Wakeham, S.G., Hinrichs, K.-U., In situ production of branched glycerol dialkyl

502 glycerol tetraethers in anoxic marine water columns. *Mar. Chem.*, 166, 1–8, 2014.

503 Loomis, S.E., Russell, J.M., Damsté, J.S.S., Distributions of branched GDGTs in soils and lake sediments  
504 from western Uganda: Implications for a lacustrine paleothermometer. *Org. Geochem.*, 42, 739–  
505 751, 2011.

506 Meyers, P.A., Organic geochemical proxies of paleoceanographic, paleolimnologic, and paleoclimatic  
507 processes. *Org. Geochem.*, 27, 213–250, 1997.

508 Milliman, J.D., Meade, R.H., World-wide delivery of river sediment to the oceans. *J. Geol.*, 91, 1-21,  
509 1983.

510 Mueller-Niggemann, C., Utami, S.R., Marxen, A., Mangelsdorf, K., Bauersachs, T., Schwark, L.,  
511 Distribution of tetraether lipids in agricultural soils–differentiation between paddy and upland  
512 management. *Biogeosciences*, 13, 1647–1666, 2016.

513 O'Brien, C.L., Foster, G.L., Martínez-Botí, M.A., Abell, R., Rae, J.W.B., Pancost, R.D., High sea surface  
514 temperatures in tropical warm pools during the Pliocene. *Nat Geosci*, 7, 606–611, 2014.

515 Peterse, F., Kim, J.-H., Schouten, S., Kristensen, D.K., Koç, N., Sinninghe Damsté, J.S., Constraints on  
516 the application of the MBT/CBT palaeothermometer at high latitude environments (Svalbard,  
517 Norway). *Org. Geochem.*, 40, 692–699, 2009a.

518 Peterse, F., Schouten, S., van der Meer, J., van der Meer, M.T.J., Sinninghe Damsté, J.S., Distribution of  
519 branched tetraether lipids in geothermally heated soils: Implications for the MBT/CBT  
520 temperature proxy. *Org. Geochem.*, 40, 201–205, 2009b.

521 Peterse, F., van der Meer, J., Schouten, S., Weijers, J.W.H., Fierer, N., Jackson, R.B., Kim, J.-H.,  
522 Sinninghe Damsté, J.S., Revised calibration of the MBT–CBT paleotemperature proxy based  
523 on branched tetraether membrane lipids in surface soils. *Geochim. Cosmochim. Acta*, 96, 215–  
524 229, 2012.

525 Peterse, F., Vonk, J.E., Holmes, R.M., Giosan, L., Zimov, N., Eglinton, T.I., Branched glycerol dialkyl  
526 glycerol tetraethers in Arctic lake sediments: Sources and implications for paleothermometry at  
527 high latitudes. *J. Geophys. Res.-Biogeo.*, 119, 1738–1754, 2014.

528 Ren, M.-E., Shi, Y.-L., Sediment discharge of the Yellow River (China) and its effect on the sedimentation  
529 of the Bohai and the Yellow Sea. *Cont. Shelf. Res.*, 6, 785–810, 1986.

530 Schouten, S., Hopmans, E.C., Baas, M., Boumann, H., Standfest, S., Konneke, M., Stahl, D.A.,  
531 Sinninghe Damste, J.S., Intact membrane lipids of "Candidatus Nitrosopumilus maritimus," a

532 cultivated representative of the cosmopolitan mesophilic group I Crenarchaeota. *Appl. Environ.*  
533 *Microbiol.*, 74, 2433–2440, 2008.

534 Schouten, S., Hopmans, E.C., Schefuß, E., Sinninghe Damsté, J.S., Distributional variations in marine  
535 crenarchaeotal membrane lipids: a new tool for reconstructing ancient sea water temperatures?  
536 *Earth Planet. Sci. Lett.*, 204, 265–274, 2002.

537 Schouten, S., Hopmans, E.C., Sinninghe Damsté, J.S., The organic geochemistry of glycerol dialkyl  
538 glycerol tetraether lipids: A review. *Org. Geochem.*, 54, 19–61, 2013.

539 Sinninghe Damsté, J.S., Spatial heterogeneity of sources of branched tetraethers in shelf systems: The  
540 geochemistry of tetraethers in the Berau River delta (Kalimantan, Indonesia). *Geochim.*  
541 *Cosmochim. Acta*, 186, 13–31, 2016.

542 Sinninghe Damsté, J.S., Hopmans, E.C., Pancost, R.D., Schouten, S., Geenevasen, J.A.J., Newly  
543 discovered non-isoprenoid glycerol dialkyl glycerol tetraether lipids in sediments. *Chem.*  
544 *Commun.*, 17, 1683–1684, 2000.

545 Sinninghe Damsté, J.S., Ossebaar, J., Abbas, B., Schouten, S., Verschuren, D., Fluxes and distribution of  
546 tetraether lipids in an equatorial African lake: Constraints on the application of the TEX<sub>86</sub>  
547 palaeothermometer and BIT index in lacustrine settings. *Geochim. Cosmochim. Acta*, 73, 4232–  
548 4249, 2009.

549 Sinninghe Damsté, J.S., Ossebaar, J., Schouten, S., Verschuren, D., Altitudinal shifts in the branched  
550 tetraether lipid distribution in soil from Mt. Kilimanjaro (Tanzania): Implications for the  
551 MBT/CBT continental palaeothermometer. *Org. Geochem.*, 39, 1072–1076, 2008.

552 Sinninghe Damsté, J.S., Rijpstra, W.I.C., Hopmans, E.C., Weijers, J.W.H., Foesel, B.U., Overmann, J.,  
553 Dedysh, S.N., 13,16-Dimethyl Octacosanedioic Acid (iso-Diabolic Acid), a Common  
554 Membrane-Spanning Lipid of Acidobacteria Subdivisions 1 and 3. *Appl. Environ. Microbiol.*,  
555 77, 4147–4154, 2011.

556 Sinninghe Damsté, J.S., Schouten, S., Hopmans, E.C., van Duin, A.C.T., Geenevasen, J.A.J.,  
557 Crenarchaeol: the characteristic core glycerol dibiphytanyl glycerol tetraether membrane lipid  
558 of cosmopolitan pelagic crenarchaeota. *J. Lipid Res.*, 43, 1641–1651, 2002.

559 Smith, R.W., Bianchi, T.S., Li, X., A re-evaluation of the use of branched GDGTs as terrestrial biomarkers:  
560 Implications for the BIT Index. *Geochim. Cosmochim. Acta*, 80, 14–29, 2012.

561 Sofianos, S.S., Johns, W.E., Murray, S.P., Heat and freshwater budgets in the Red Sea from direct

562 observations at Bab el Mandeb. *Deep Sea Res. Part II: Top. Stud. Oceanogr.*, 49, 1323–1340,  
563 2002.

564 Sparkes, R.B., Doğrul Selver, A., Bischoff, J., Talbot, H.M., Gustafsson, Ö., Semiletov, I.P., Dudarev,  
565 O.V., van Dongen, B.E., GDGT distributions on the East Siberian Arctic Shelf: implications for  
566 organic carbon export, burial and degradation. *Biogeosciences*, 12, 3753–3768, 2015.

567 Taylor, K.W.R., Huber, M., Hollis, C.J., Hernandez-Sanchez, M.T., Pancost, R.D., Re-evaluating modern  
568 and Palaeogene GDGT distributions: Implications for SST reconstructions. *Glob. Planet.*  
569 *Change*, 108, 158-174, 2013.

570 Tierney, J.E., Russell, J.M., Distributions of branched GDGTs in a tropical lake system: Implications for  
571 lacustrine application of the MBT/CBT paleoproxy. *Org. Geochem.*, 40, 1032–1036, 2009.

572 Tierney, J.E., Schouten, S., Pitcher, A., Hopmans, E.C., Sinninghe Damsté, J.S., Core and intact polar  
573 glycerol dialkyl glycerol tetraethers (GDGTs) in Sand Pond, Warwick, Rhode Island (USA):  
574 Insights into the origin of lacustrine GDGTs. *Geochim. Cosmochim. Acta*, 77, 561–581, 2012.

575 Trommer, G., Siccha, M., Meer, M.T.J.V.D., Schouten, S., Damsté, J.S.S., Schulz, H., Hemleben, C.,  
576 Kucera, M., Distribution of Crenarchaeota tetraether membrane lipids in surface sediments from  
577 the Red Sea. *Org. Geochem.*, 40, 724–731, 2009.

578 Walsh, E.M., Ingalls, A.E., Keil, R.G., Sources and transport of terrestrial organic matter in Vancouver  
579 Island fjords and the Vancouver-Washington Margin: A multiproxy approach using  $\delta^{13}\text{C}_{\text{org}}$ ,  
580 lignin phenols, and the ether lipid BIT index. *Limnol. Oceanogr.*, 53, 1054–1063, 2008.

581 Weijers, J.W.H., Schefuß, E., Kim, J.-H., Sinninghe Damsté, J.S., Schouten, S., Constraints on the  
582 sources of branched tetraether membrane lipids in distal marine sediments. *Org. Geochem.*, 72,  
583 14–22, 2014.

584 Weijers, J.W.H., Schefuß, E., Schouten, S., Damsté, J.S.S., Coupled Thermal and Hydrological Evolution  
585 of Tropical Africa over the Last Deglaciation. *Science*, 315, 1701–1704, 2007a.

586 Weijers, J.W.H., Schouten, S., Donker, J.C.V.D., Hopmans, E.C., Damsté, J.S.S., Environmental controls  
587 on bacterial tetraether membrane lipid distribution in soils. *Geochim. Cosmochim. Acta*, 71,  
588 703–713, 2007b.

589 Weijers, J.W.H., Schouten, S., Spaargaren, O.C., Sinninghe Damsté, J.S., Occurrence and distribution of  
590 tetraether membrane lipids in soils: Implications for the use of the  $\text{TEX}_{86}$  proxy and the BIT  
591 index. *Org. Geochem.*, 37, 1680–1693, 2006.

592 White, D.C., Davis, W.M., Nickels, J.S., King, J.D., Bobbie, R.J., Determination of the sedimentary  
593 microbial biomass by extractible lipid phosphate. *Oecologia*, 40, 51–62, 1979.

594 Wu, W., Ruan, J., Ding, S., Zhao, L., Xu, Y., Yang, H., Ding, W., Pei, Y., Source and distribution of  
595 glycerol dialkyl glycerol tetraethers along lower Yellow River-estuary–coast transect. *Mar.*  
596 *Chem.*, 158, 17–26, 2014.

597 Wu, W., Zhao, L., Pei, Y., Ding, W., Yang, H., Xu, Y., Variability of tetraether lipids in Yellow River-  
598 dominated continental margin during the past eight decades: Implications for organic matter  
599 sources and river channel shifts. *Org. Geochem.*, 60, 33–39, 2013.

600 Xiao, W., Xu, Y., Ding, S., Wang, Y., Zhang, X., Yang, H., Wang, G., Hou, J., Global calibration of a  
601 novel, branched GDGT-based soil pH proxy. *Org. Geochem.*, 89, 56–60, 2015.

602 Yang, G., Zhang, C.L., Xie, S., Chen, Z., Gao, M., Ge, Z., Yang, Z., Microbial glycerol dialkyl glycerol  
603 tetraethers lipids from water and soil at the Three Gorges Dam on the Yangtze River. *Org.*  
604 *Geochem.*, 56, 40–50, 2013.

605 Yang, H., Pancost, R.D., Dang, X., Zhou, X., Evershed, R.P., Xiao, G., Tang, C., Gao, L., Guo, Z., Xie,  
606 S., Correlations between microbial tetraether lipids and environmental variables in Chinese soils:  
607 Optimizing the paleo-reconstructions in semi-arid and arid regions. *Geochim. Cosmochim. Acta*,  
608 126, 49–69, 2014a.

609 Yang, H., Pancost, R.D., Tang, C., Ding, W., Dang, X., Xie, S., Distributions of isoprenoid and branched  
610 glycerol dialkanol diethers in Chinese surface soils and a loess–paleosol sequence: Implications  
611 for the degradation of tetraether lipids. *Org. Geochem.*, 66, 70–79, 2014b.

612 Zell, C., Kim, J.-H., Dorhout, D., Baas, M., Sinninghe Damsté, J.S., Sources and distributions of  
613 branched tetraether lipids and crenarchaeol along the Portuguese continental margin:  
614 Implications for the BIT index. *Cont. Shelf. Res.*, 96, 34–44, 2015.

615 Zell, C., Kim, J.-H., Hollander, D., Lorenzoni, L., Baker, P., Silva, C.G., Nittrouer, C., Sinninghe Damsté,  
616 J.S., Sources and distributions of branched and isoprenoid tetraether lipids on the Amazon shelf  
617 and fan: Implications for the use of GDGT-based proxies in marine sediments. *Geochim.*  
618 *Cosmochim. Acta*, 139, 293–312, 2014.

619 Zhang, Y.G., Zhang, C.L., Liu, X.-L., Li, L., Hinrichs, K.-U., Noakes, J.E., Methane Index: A tetraether  
620 archaeal lipid biomarker indicator for detecting the instability of marine gas hydrates. *Earth*  
621 *Planet. Sci. Lett.*, 307, 525–534, 2011.

622 Zhu, C., Wakeham, S.G., Elling, F.J., Basse, A., Mollenhauer, G., Versteegh, G.J.M., Ouml, nneke, M.,  
623 Hinrichs, K.U., Stratification of archaeal membrane lipids in the ocean and implications for  
624 adaptation and chemotaxonomy of planktonic archaea. *Environ. Microbiol.*, DOI:  
625 10.1111/1462-2920.13289, 2016.

626 Zhu, C., Weijers, J.W.H., Wagner, T., Pan, J.M., Chen, J.F., Pancost, R.D., Sources and distributions of  
627 tetraether lipids in surface sediments across a large river-dominated continental margin. *Org.*  
628 *Geochem.*, 42, 376–386, 2011.

629

630

631

632

633

634

635

636

637

638

639

640

641

642

643

644

645

646

647

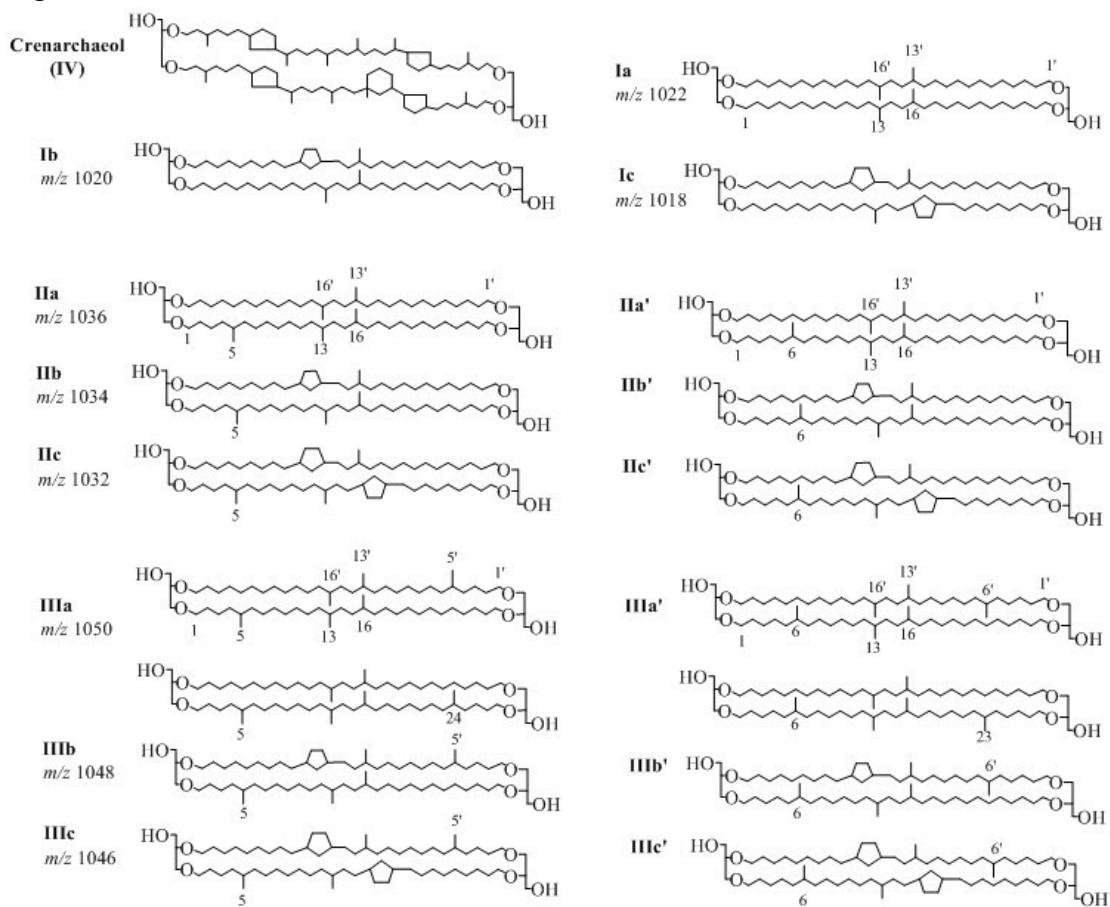
648

649

650

651

652 Fig.1. Chemical structures of branched GDGTs and crenarchaeol.



653

654

655

656

657

658

659

660

661

662

663

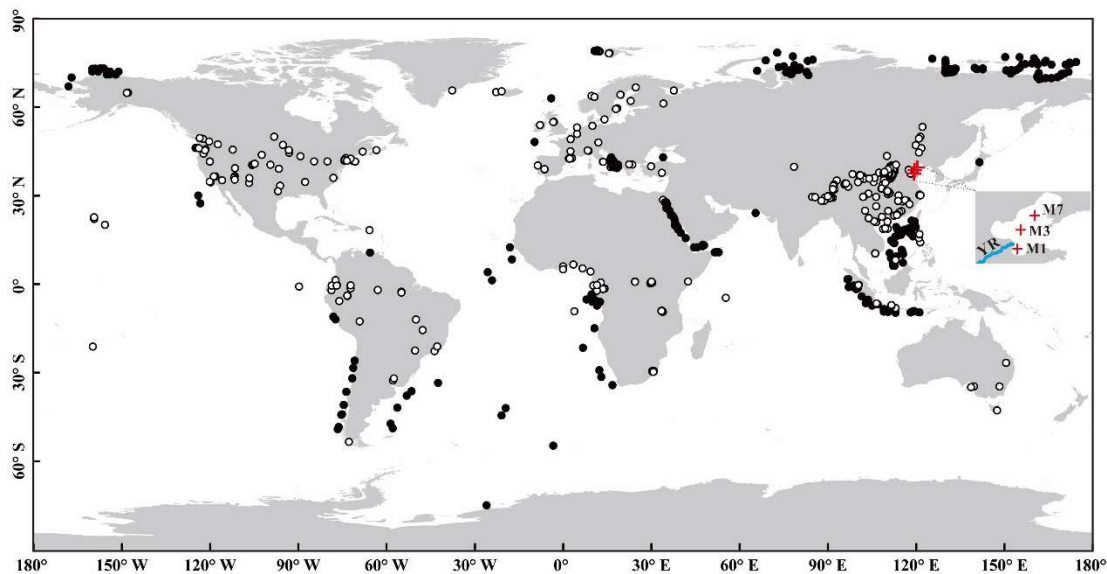
664

665

666

667

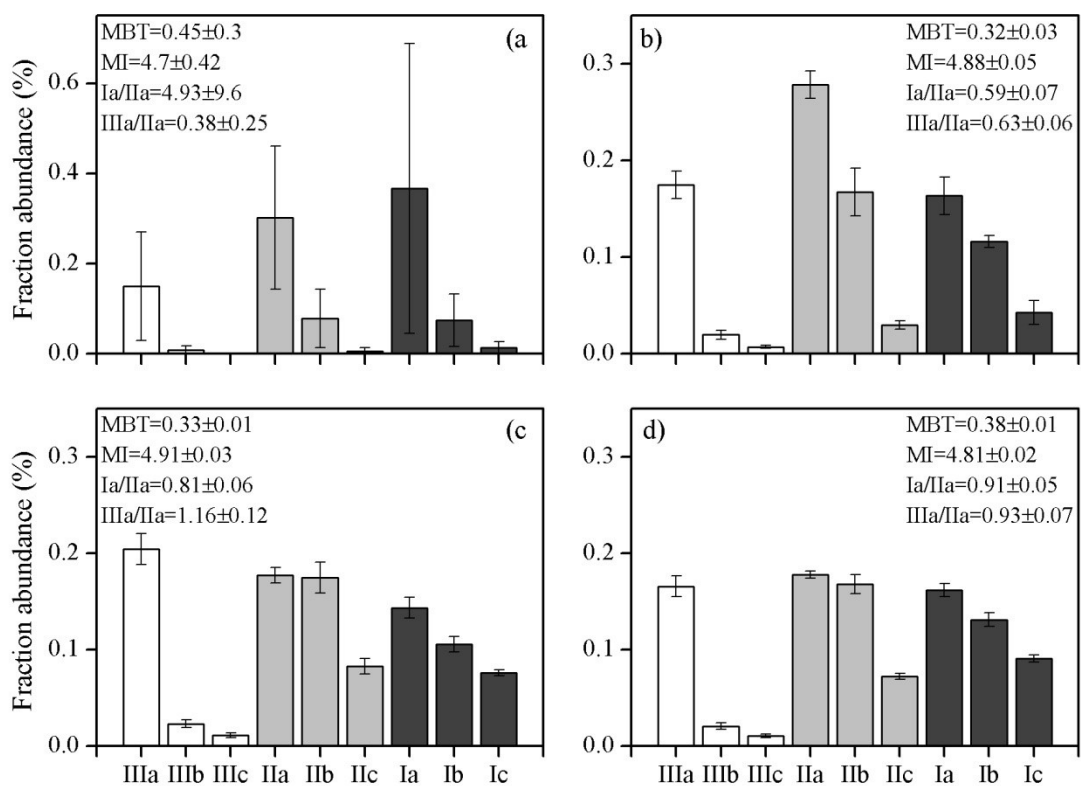
668 Fig.2. Location of the samples used in this study. White circles and black circles  
669 indicate the soils and marine sediments, respectively. Red crosses denote three sediment  
670 cores (M1, M3 and M7) in the Bohai Sea. YR is the Yellow River.



671  
672  
673  
674  
675  
676  
677  
678  
679  
680  
681  
682  
683  
684  
685  
686  
687  
688

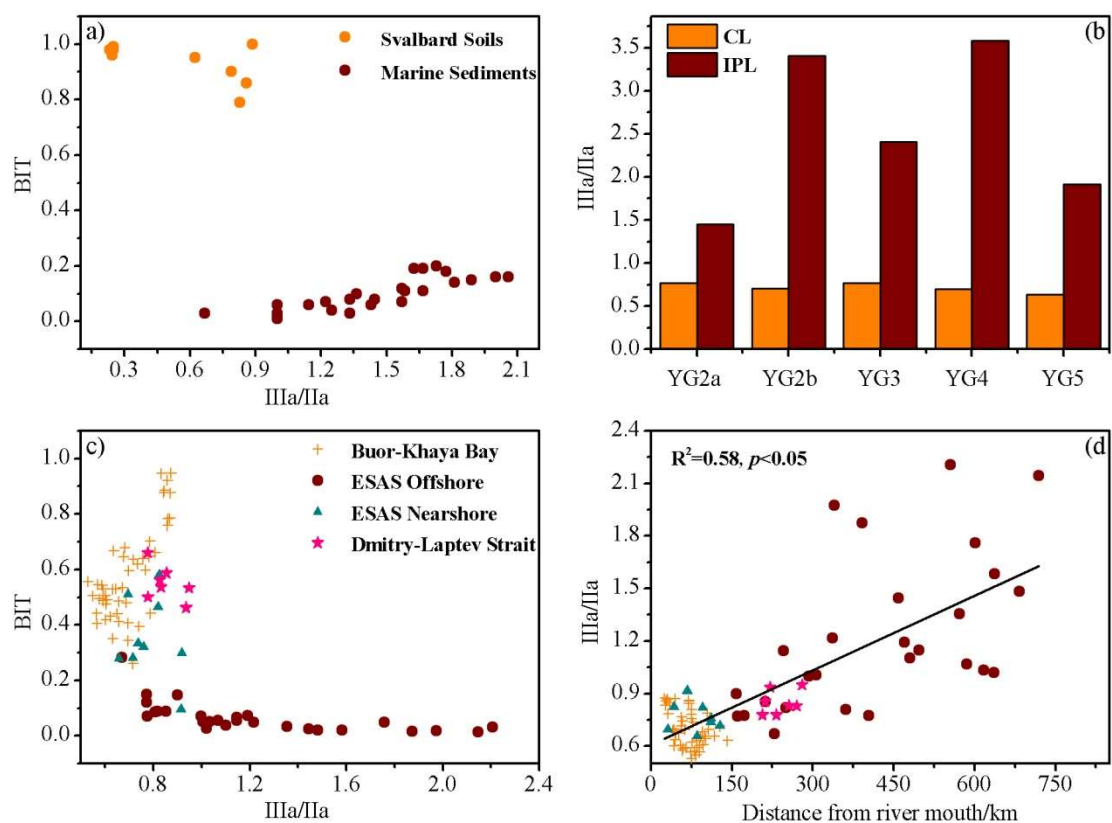


689 Fig.3. Averaged percentages of individual brGDGTs in soils (a), core M1 (b), M3 (c)  
 690 and M7 (d). The soil data are from Yang et al. (2014a).



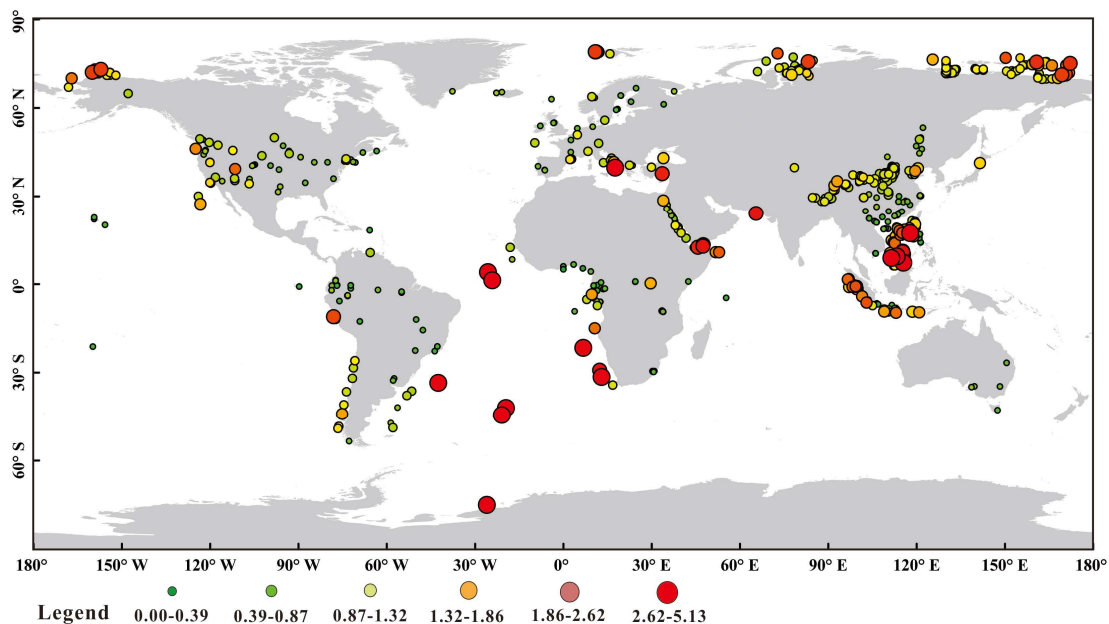
691  
 692  
 693  
 694  
 695  
 696  
 697  
 698  
 699  
 700  
 701  
 702  
 703  
 704  
 705

706 Fig. 4. a) The relationship between brGDGT IIIa/IIa ratio and the BIT index of samples  
 707 from Peterse et al. (2009a); b) histograms of brGDGT IIIa/IIa ratio of the core lipids  
 708 (CLs) and intact polar lipids (IPLs) in samples from De Jonge et al. (2015); c) the  
 709 relationship between brGDGT IIIa/IIa ratio and the BIT index in samples from Sparkes  
 710 et al. (2015); d) the relationship between brGDGT IIIa/IIa ratio and distance from river  
 711 mouth in samples from Sparkes et al. (2015).



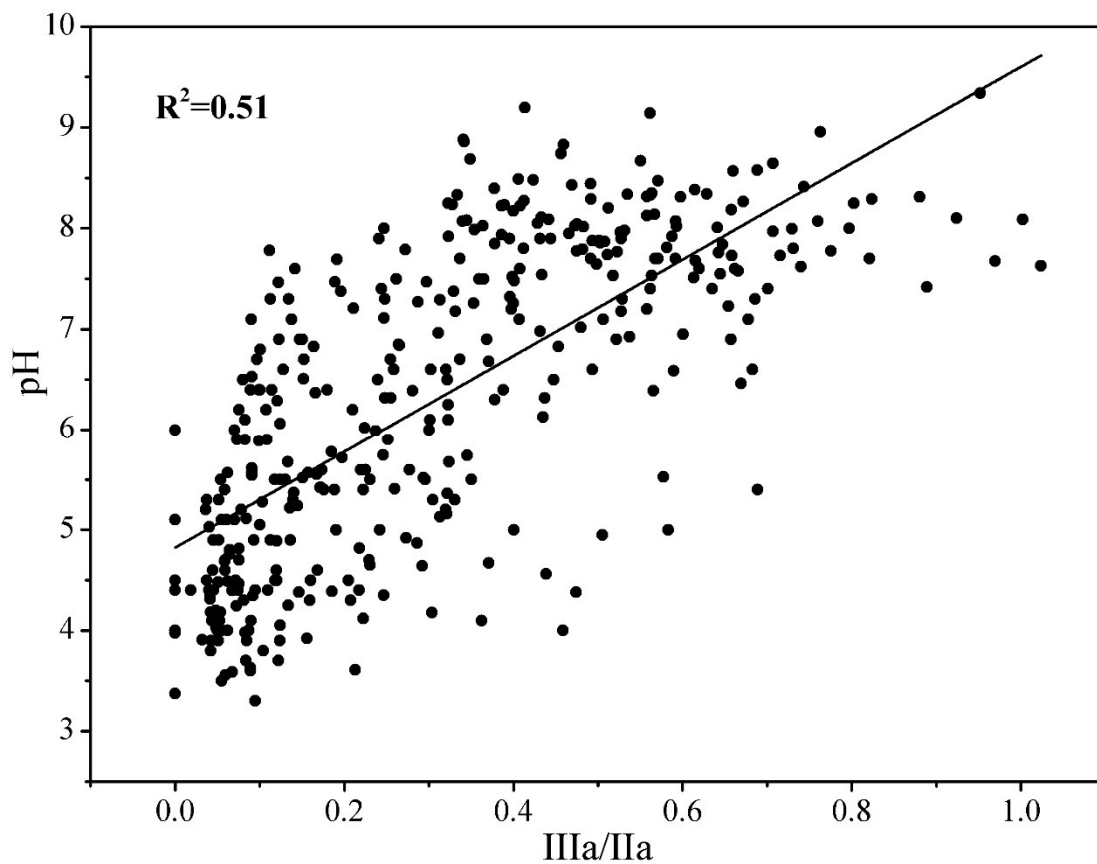
712  
 713  
 714  
 715  
 716  
 717  
 718  
 719  
 720  
 721  
 722

723 Fig. 5. Global distribution pattern of brGDGT IIIa/IIa ratio in soils and marine  
724 sediments.



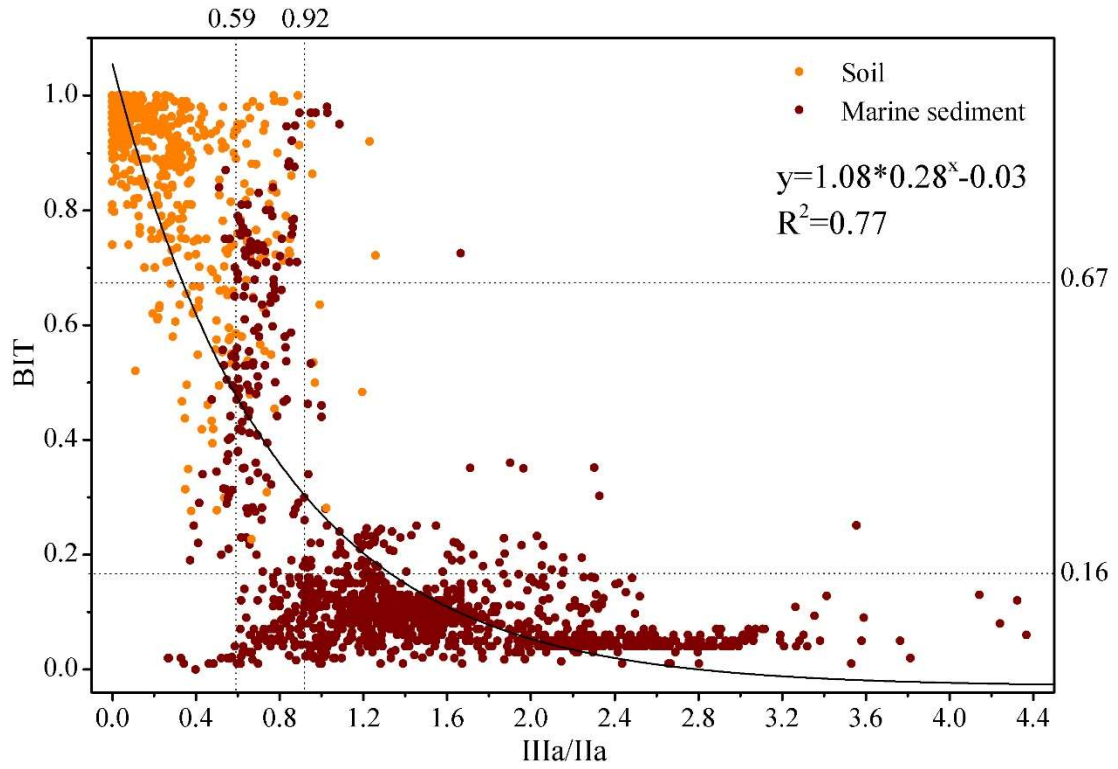
725  
726  
727  
728  
729  
730  
731  
732  
733  
734  
735  
736  
737  
738  
739  
740  
741  
742  
743

744 Fig. 6 a plot showing a positive correlation between soil pH and IIIa/IIa. The data are from  
745 Peterse et al. (2012) and this study.



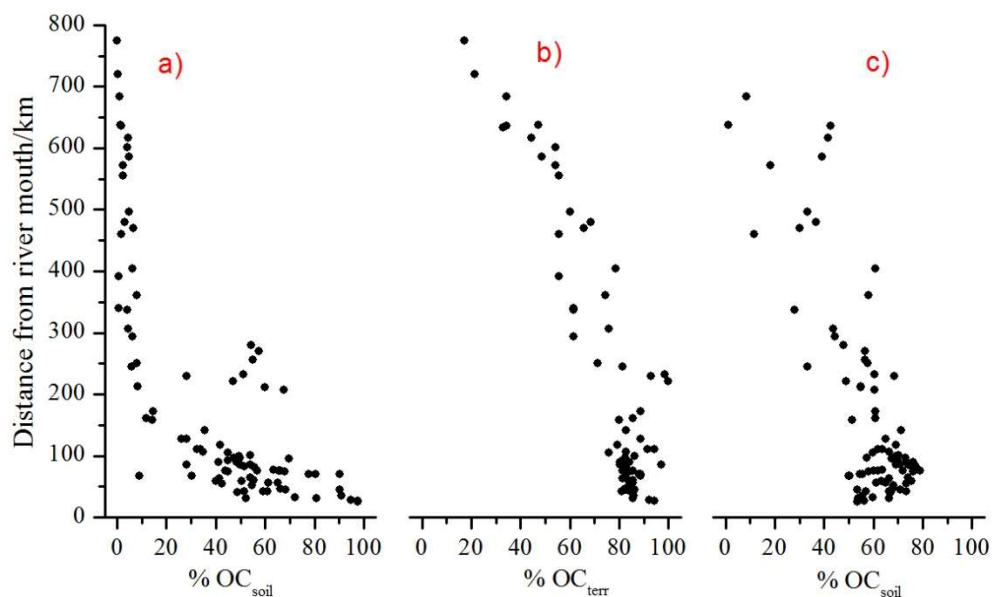
746  
747  
748  
749  
750  
751  
752  
753  
754  
755  
756  
757  
758  
759  
760

761 Fig. 7. Relationship between the IIIa/IIa ratio and the BIT index of globally distributed  
762 samples: soils (orange circle) and marine sediments (red circle). Dashed lines represent  
763 lower or upper threshold values for 90% of soils/sediments.



764  
765  
766  
767  
768  
769  
770  
771  
772  
773  
774  
775  
776  
777  
778

779 Fig. 8. Percentage of soil organic carbon (%OC<sub>soil</sub>) or terrestrial organic carbon  
780 (%OC<sub>terr</sub>) based on a binary mixing model of BIT (a),  $\delta^{13}\text{C}_{\text{org}}$  (b) and IIIa/IIa (c) for the  
781 East Siberian Arctic Shelf (Sparkes et al., 2015).



782

783

784

785

786

787

788

789

790

791

792

793

794

795

796

797

798

799

800 Table 1: Parameters including brGDGTs IIIa/IIa, Ia/IIa, the BIT index, MBT, MI, DC,  
 801 percentages of tetra-, penta- and hexa-methylated brGDGTs, and the weighted average  
 802 number of cyclopentane moieties (#rings for tetramethylated brGDGTs) based on the  
 803 GDGTs from three cores (M1, M3 and M7; see figure 2) in the Bohai Sea. Different  
 804 letters in parenthesis (a, b, c, d) represent significant difference at the level of  $p < 0.05$ .

Indexes	Soil	M1	M3	M7
IIIa/IIa	0.39±0.25 (a)	0.63±0.06 (b)	1.16±0.12 (c)	0.93±0.07 (d)
Ia/IIa	4.93±9.60 (a)	0.59±0.07 (b)	0.81±0.06 (b)	0.91±0.05 (b)
BIT	0.75±0.22 (a)	0.50±0.19 (b)	0.14±0.06 (c)	0.11±0.03 (c)
MBT	0.45±0.30 (a)	0.32±0.03 (b)	0.33±0.01 (b)	0.38±0.01 (ab)
MI	4.70±0.42 (a)	4.88±0.05 (b)	4.91±0.03 (b)	4.81±0.02 (ab)
DC	0.31±0.21 (a)	0.62±0.03 (b)	0.79±0.03 (c)	0.82±0.02 (c)
%tetra	0.45±0.30 (a)	0.32±0.03 (b)	0.33±0.01 (c)	0.38±0.01 (c)
%hexa	0.16±0.12 (a)	0.20±0.02 (b)	0.24±0.02 (b)	0.20±0.01 (b)
%penta	0.39±0.20 (a)	0.48±0.02 (b)	0.44±0.02 (b)	0.42±0.01 (b)
#Rings <sub>Stera</sub>	0.20±0.15 (a)	0.39±0.03 (b)	0.47±0.02 (c)	0.47±0.02 (c)

805

806